Journal of Stress Analysis
Vol. 1, No. 2, Autumn – Winter 2016-17
Bu-Ali Sina University

Evaluation Effects of Modeling Parameters on the Temperature Fields and Residual Stresses of Butt-Welded Stainless Steel Pipes

S. Feli*, M.E. Aalami Aaleagha, M.R. Jahanban
Mechanical Engineering Department, Razi University, Kermanshah, Iran.

Article info

Article history:
Received 2016.07.22
Received in revised form
2016.10.31
Accepted 2017.02.13

Keywords:
Residual stress
Butt-welded
Stainless steel pipe
Temperature field

Abstract

In this paper, the effects of modeling parameters on the temperature field and residual stresses of butt-welded stainless steel pipes were investigated by using finite element modeling in ABAQUS code. The investigated parameters included, heat flux distribution, latent heat, and heat flux type. The birth and death techniques were utilized to consider mass addition from Y308L filler metal into the weld pool. The moving heat source and convection heat transfer were also modeled by a user subroutine DFLUX and FILM in ABAQUS code. In this work, for verification of FE modeling the temperature fields and residual stresses were compared with available experimental results. The simulation results showed that heat flux with a double ellipsoidal distribution proposed by Goldak associated with latent heat parameter and employed a fully volumetric arc heat input, representing the best match with the experimental data.

1. Introduction

Fusion welding is a joining process in which the coale scence of metals is achieved by fusion. This form of welding is widely employed in fabricating structures such as ships, offshore structures, steel bridges, and pressure vessels. Owing to localized heating by the welding process and subsequent rapid cooling, residual stresses can arise in the weld itself and in the base metal. Residual stresses attributed to welding pose significant problems in the accurate fabrication of structures because those stresses heavily induce brittle fracturing and degrade the buckling strength of welded structures. Residual stresses during welding are unavoidable and their effects on welded structures cannot be disregarded. Design and fabrication conditions, such as the structure thickness, joint design, welding conditions and welding sequence, must be altered so that the adverse effects of residual stresses can be reduced to acceptable levels. Therefore, estimating the magnitude and distribution of welding residual stresses and characterizing the effects of certain welding conditions on the residual stresses are particularly important.

In the last decade several FE models have been proposed to predict temperature fields and residual stresses in multi-pass butt-welded steel pipes.

Deng and Murakawa [1] compared the numerical simulated results of both the temperature field and the welding residual stress field with experimental measurements for stainless steel pipes. The 2D axisymmetricand 3D models were also developed. The results showed that a 2D axisymmetric model can also give a reasonable prediction for both the temperature field and the residual stress field in stainless steel pipe except for the welding start-finish location.

Brickstad and Josefson [2] employed a 2D axisymmetricmodel to numerically simulate a series of multi-pass circumferential butt-weldingof stainless steel pipe in a non-linear thermo mechanical FE analysis. Tso-Liang et al. [3] evaluated the residual stresses with various types of welding sequence in single pass, multi pass

*Corresponding author: S. Feli (Associate Professor)
E-mail address: Felisaeid@razi.ac.ir

butt-welded plates and circular patch welds. This investigation has provided an available welding sequence to enhance the fabrication process of welded structures.

Lee and Chang [4] presented parametric studies with inside radius to wall thickness ratio ranging from 10 to 100 to investigate the effects of pipe diameter on residual stresses. Sattari-far and Farahani [5] investigated the effects of the weld groove shape and pass number on residual stresses in butt-welded pipes. It was shown that these two parameters may have significant effects on magnitude and distribution of residual stresses in welded pipes.

Feli et al. [6] used the 3D and 2D axisymmetric FE model to investigate the welding temperature field and the residual stress distribution for thin-walled pipes. Also the effects of welding sequences on the thermal and structural analysis were investigated. Four types of welding sequences for circular welds of pipe were used and concluded that except the starting point of welding, there are no important differences of axial and hoop residual stresses for welding sequences.

Foroutan et al. [7], investigated the effect of hydrostatic testing internal pressure on the residual stresses of circumferentially butt-welded steel pipes by a three-dimensional finite element simulation. The results obtained from this study showed that the hydrostatic testing pressure has a significant effect on residual stresses.

In this study, a 3D finite element simulation was developed to investigate the distribution of temperature fields and residual stresses during two-pass tungsten inert gas arc welding in a stainless steel pipe. In this numerical simulation, the uncoupled thermal-mechanical model, the temperature dependent thermal-physical properties and the add and remove elements in the thermal and structural analysis, were utilized. The effects of heat flux distribution, latent heat, and heat flux type on temperature fields and residual stresses were also investigated and temperature fields axial and hoop residual stresses were compared.

2. FE Simulation of the Welding Process

In this section by using ABAQUS 6.8-1 software, a 3D thermal elastic-plastic FE computational procedure was employed to simulate the welding temperature fields and residual stresses in stainless steel pipe. The analysis included two steps. The first step was that the heat conduction problem which was solved independently from the thermal analysis to obtain the temperature distribution with time and space and in the second step the temperature history in each node was employed as the thermal load in the subsequent mechanical analysis and distribution of stresses in pipe was determined. The temperature-dependent thermal-physical properties of SUS304 stainless steel pipe such as specific heat, conductivity, density, and temperature-dependent thermal-mechanical properties including young's modulus, Poisson's ratio, thermal expansion coefficient, and yield strength were used for thermal analysis and mechanical analysis respectively. The thermal and mechanical properties of SUS304 areshown in Table 1. In this paper based on the reference [8], the mechanical properties of weld metal were assumed to be the same as base metal.

The 3D finite element model of pipe with 22000 brick elements is shown in Fig. 1. Also the welding arc travel direction and welding start/stop position ($\theta = 0^\circ$) is shown in the Fig. 1. Because of the symmetry, one half of the model was selected as the analysis model, which had a fine grid in the welding zone. The smallest element was $3.5 \times 1.5 \times 0.8$mm. The length, the outer diameter and the thickness of the pipe were 400mm, 114.3mm and 6mm, respectively.

Table 1
Thermal physical properties and mechanical properties of SUS304 [1].

Temperature °C	Specific heat J/g°C	Conductivity j/mm°Cs	Density gr/mm^3	Yield stress MPa	Thermal expansion °C^{-1}	Young's modulus GPa	Poisson's ratio
0	0.462	0.0146	0.79	265	1.7e-5	198	0.294
100	0.496	0.151	0.788	218	1.74e-5	193	0.295
200	0.512	0.0161	0.783	186	1.8e-5	185	0.301
300	0.525	0.0179	0.779	170	1.86e-5	176	0.310
400	0.540	0.0180	0.775	155	1.91e-5	167	0.318
600	0.577	0.0208	0.766	149	1.96e-5	159	0.326
800	0.604	0.0239	0.756	91	2.02e-5	151	0.333
1200	0.676	0.0322	0.737	25	2.07e-5	60	0.339
1300	0.692	0.0337	0.732	21	2.11e-5	20	0.342
1500	0.7	0.12	0.732	10	2.1e-5	10	0.338

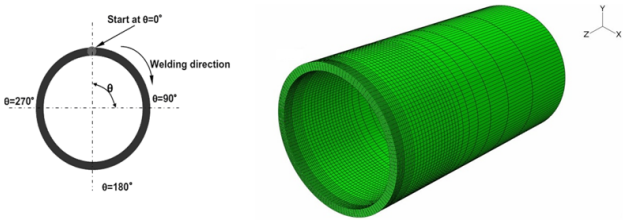

Fig. 1. 3D finite element model and welding direction.

2.1. Thermal Analysis

The 8-node 3D thermal element DC3D8 with a single degree of freedom was employed for both the base and weld metal. The pipe was welded by 2-pass welding process; the technique of element addition and removal was adopted to simulate the weld filler variation with time in multi-pass butt-welded piping. All elements had tobe created, including those welds fillers to be born in later stages, and new elements were added to the mesh periodically after the previous pass was completed.

In this study, the heat from the moving welding arc was applied as a volumetric heat source with a double ellipsoidal distribution proposed by Goldak John and Akhlaghi [9] and is expressed by the following equations:
For the front heat source:

$$q_r = (x, y, z, t) = \frac{6\sqrt{3} f_f Q}{abc_f \pi \sqrt{\pi}} e^{-x^2/a^2} e^{-3y^2/b^2} e^{-3z^2/c_f^2} \tag{1}$$

For the rear heat source:

$$q_r(x, y, z, f) = \frac{6\sqrt{3} f_r Q}{abc_r \pi \sqrt{\pi}} e^{-x^2/a^2} e^{-3y^2/b^2} e^{-3z^2/c_r^2} \tag{2}$$

where x, y and z are the local coordinates of the double ellipsoid model aligned with the welded pipe; f_f respectively. In this paper, it was assumed that $f_r = 1.4$, $f_r = 0.6$ [8].

Q is the power of the welding heat source which can be calculated according to the welding current, the arc voltage, and the arc efficiency. The arc efficiency was assumed to be 70% for the TIG welding process.

The parameters a, b, c_f, c_r are related to the characteristics of the welding heat source. The parameters of the heat source can be adjusted to create a desired melted zone according to the welding conditions.

The welding condition and the numerical values of heat source parameters (a, b, c_f, c_r) of SUS304 stainless steel pipe for each pass are presented in Tables 2 and 3, respectively. The highest temperature of the weld pool is about 2200°C. To account for heat transfer, due to fluid flow in the weld pool, an artificially increased thermal conductivity which is several times larger than the value at room temperature is assumed for temperatures above the melting point. The liquid-to-solid phase transformation effects of the weld pool were modeled by taking into account the latent heat of fusion. The latent heat, the heat energy that the system stores and releases during the phase change, was assumed to be 260J/gr between the solid temperature of 1340°C and the liquid temperature of 1390°C [2]. The moving heat source was modeled by ABAQUS user subroutine DFLUX in ABAQUS code.

Table 2
Welding condition for each pass [1].

Pass Number	Arc voltage (V)	Welding current (A)	Welding speed mm/min
1	9.5	140	80
2	9.5	160	80

Table 3
The numerical values of the heat source parameters [9].

Parameters of the heat source (mm)				Pass Number
c_r	c_f	b	a	
6	1.5	4	3	1
7	1.75	3.5	3.5	2

As for the boundary conditions applied to the thermal model, convection and radiation were both taken into account and their combined effects are represented via the following equation for the total temperature-dependent heat transfer coefficient, h [7]:

$$h = \begin{cases} 0.0668T \ W/m^2 & 0 < T < 500°C \\ 0.231T - 82.1 \ W/m^2 & T > 500°C \end{cases} \tag{3}$$

An ABAQUS user subroutine FILM was developed to simulate the combined thermal boundary condition. In this simulation welding time at first pass was 255.17 s and cooling time after completion of first welding passwas 1800s. Furthermore, welding time at second pass was 269.31s.

2.2. Mechanical Analysis

The same finite element model used in the thermal analysis was employed here, except for the element type and the boundary conditions. The solid element type used in the mechanical analysis wasan 8-node bi-quadratic stress/displacement quadrilateral with reduced integration (C3D8R). Because of the symmetry of the FE model and reduction of computational time, one half of the model was selected as the analysis model. Therefore a symmetry condition for weld surface relative to axis of pipe (z) was considered. The mechanical analysis was conducted using the temperature histories computed by the thermal analysis as the input data.

In the mechanical analysis, the elastic behavior was modeled using the isotropic Hook's law with

temperature-dependent young's modulus and Poisson's ratio. The thermal strain wasconsidered using the temperature-dependent thermal expansion coefficient. For the plastic behavior, a rate-independent plastic model was used.

3. Simulation Results

3.1. The Results of Thermal Analysis

At first, the temperature history was compared with the experimental results of reference [1]. In those experiments, the thermal cycles at several locations on inside and outside surfaces have been measured using the thermo-couples. Fig. 2 shows the thermal cycles at 3, 8 and 13mm from the weld bead on the inside surface where circumferential angle θ is 180°.
Fig. 2 shows the thermal history at 3mm from the weld bead of the numerical simulations has good agreement with the experimental results of reference [1].

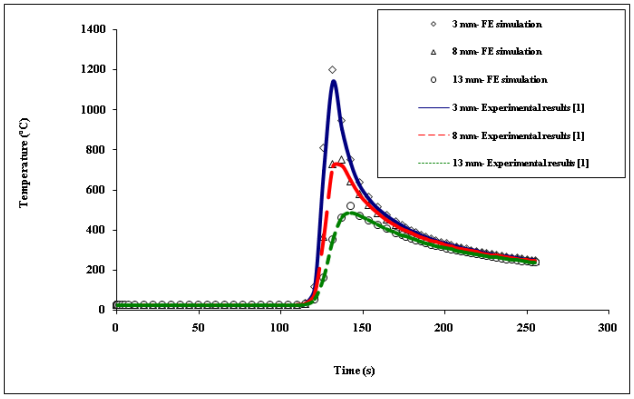

Fig. 2. Thermal history at 3, 8 and 13mm from weld bead on the inside surface after the first welding where circumferential angle θ is 180°.

The thermal cycles from 3mm from the weld bead at different circumferential locations on the inside surface during the first welding pass is plotted in Fig. 3. It is clear that the temperature histories at the three locations on the inside surface are almost identical. Therefore, it can be concluded that the temperature field is very steady when the welding torch moves around the pipe.

3.2. The Results of the Mechanical Analysis

In this section, the residual stresses of 3D FE simulation were compared with the experimental results of reference [1]. In the experiments of reference [1] after completion of welding, the strain gauges with 1mm length were used to measure the welding residual stresses. Figs. 4 and 5 show the distribution of axial and hoop residual stresses after completion of welding, respectively.

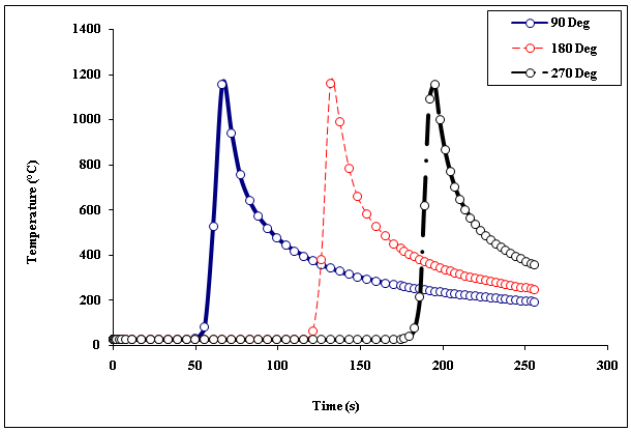

Fig. 3. Thermal cycles at 3mm from the weld bead in 90°, 180°, and 270° locations on the inside surface during the first welding.

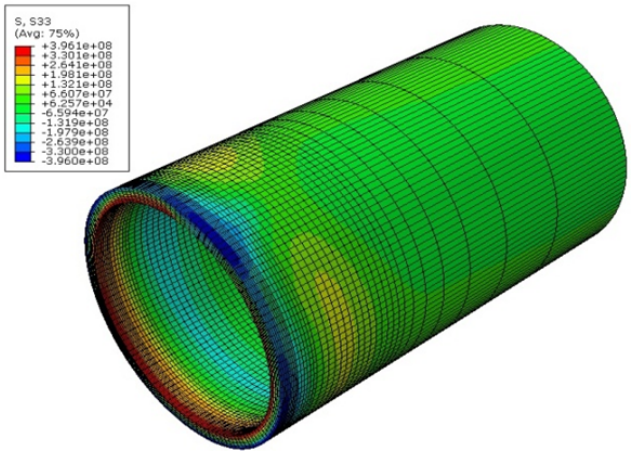

Fig. 4. Axial residual stress distribution of the welded pipe in 3D FE simulation.

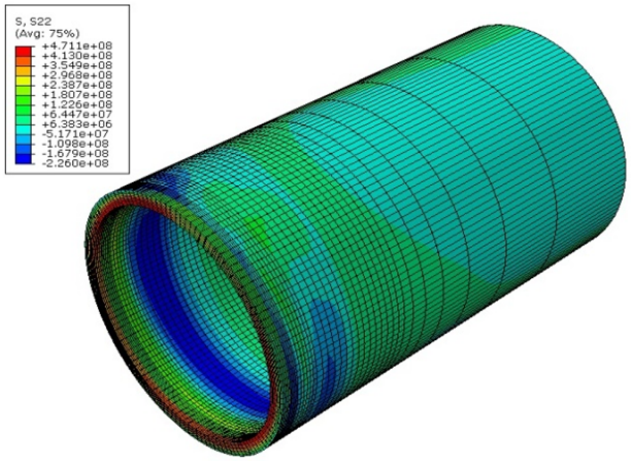

Fig. 5. Hoop residual stress distribution of the welded pipe in 3D FE simulation.

Figs. 6 and 7 show the axial residual stresses along axial direction at 180° on inside and outside surfaces, respectively. Fig. 8 shows the hoop residual stresses on

the inside surfaces along the axial direction. The black spots represent the results of the experimental value measured by strain gauges by Deng and Murakawa [1]. It is clear that the values of axial stresses in inside and outside surfaces have acceptable agreement with experimental results.

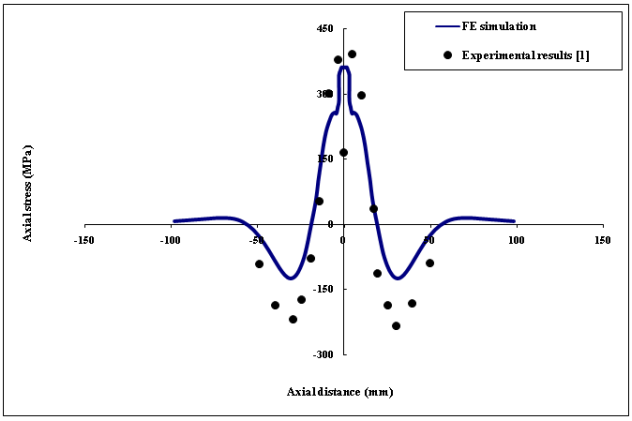

Fig. 6. Axial residual stress along axial direction inlocations with 180° on the inside surface.

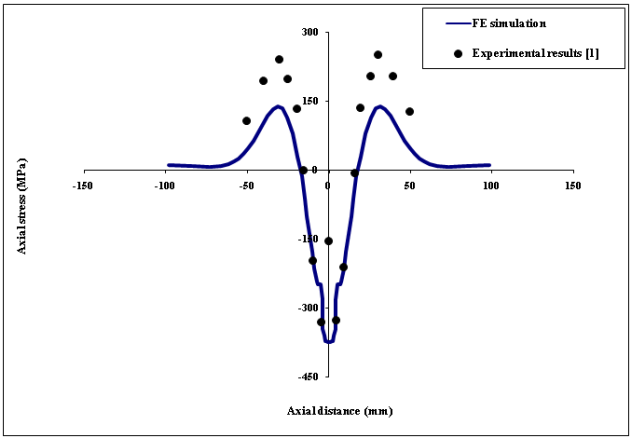

Fig. 7. Axial residual stress along axial direction inlocations with 180° on the outside surface.

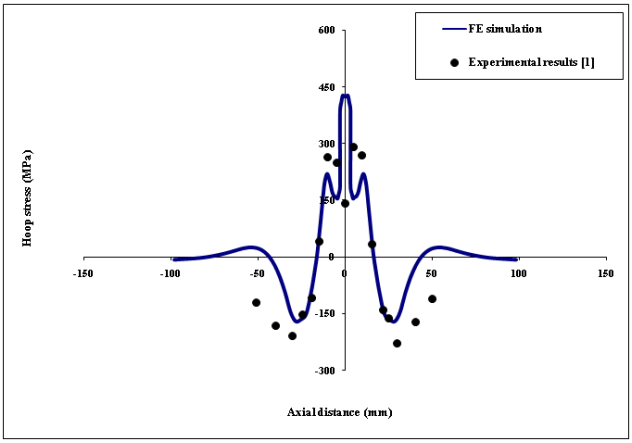

Fig. 8. Hoop residual stress distribution inlocations with 180° on the inside surface.

In the weld zone, because of high yield strength of the weld metal, the final welding axial and hoop residual stresses are much larger.

From the results, it can be observed that within and near the weld area, the axial residual stresses were tensile on the inner surface and compressive on the outer surface. This was because the local inward deformation in the vicinity of the weld region due to the circumferential shrinkage during the welding process which generates bending moment.

4. Effects of Heat Flux Distribution on Temperature Field and Residual Stresses

In this section the effects of heat flux distribution on temperature filed and residual stresses were investigated. Three types of heat flux distribution including, Goldak, ellipsoidal and spherical were considered in this paper [9].

The numerical values of the heat source parameters from Table 3 were used to simulate dimensions of weld pool in Goldak heat flux distribution. For modeling ellipsoidal heat flux distribution, dimensions of weld pool and Goldak model were deemed to be similar; only the large diagonal of ellipsoidal was assumed to equal $(c_f + c_r)/2$. In spherical heat flux distribution, three dimensions ofweld pool were assumed to equal penetration depth of weld.

4.1. Effect of Heat Flux Distribution on Temperature Field

In Fig. 9, temperature history on weld line for different types of heat flux distribution during the second welding passis showen. Also in Table 4, the magnitude of maximum temperature of pipe for different types of heat flux distribution is compared with experimental results.

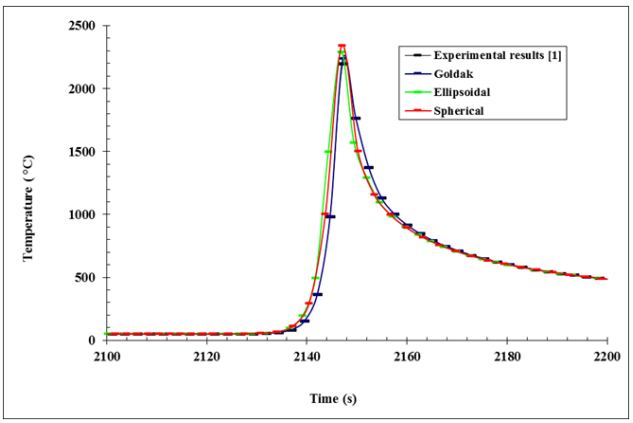

Fig. 9. Temperature history of different types of heat flux distribution during second welding pass on weld line.

Table 4
Comparison of maximum temperature on weld line for different types of heat flux distribution during second welding pass with experimental results [1].

Heat flux distribution	Maximum temperature (°C)
Goldak	2242
Ellipsoidal	2289
Spherical	2340
Experimental result [1]	2200

From Table 4, it can be observed that maximum temperature in Goldak model has good agreement with experimental results. Therefore Goldak heat source distribution has more accurately prediction of maximum temperature. Also the prediction of maximum temperature on weld line by spherical heat source distribution is more than other models. In spherical heat source distribution the dimensions of melted zone is smaller than other models.

4.2. Effect of Heat Flux Distribution on Residual Stresses

In Table 5, the values of maximum tensile and compressive axial and hoop residual stresses on the outside (OD) and inside (ID) surfaces of pipe for three types of heat flux is shown, where TAS and CAS are the tensile and compressive axial stresses, and THS and CHS are the tensile and compressive hoop stresses, respectively.

Table 5
Effect of heat flux distribution on residual stresses.

Heat flux distribution	TAS-ID (MPa)	CAS-ID (MPa)	THS-ID (MPa)
Goldak	361	-124	422
Ellipsoidal	360	-124	423
Spherical	360	-123	423

Heat flux distribution	CHS-ID (MPa)	TAS-OD (MPa)	CAS-OD (MPa)	THS-OD (MPa)	CHS-OD (MPa)
Goldak	-172	137	-379	30.2	-179
Ellipsoidal	-170	138	-377	30.5	-180
Spherical	-170	137	-377	30.5	-180

From the values of residual stresses presented in Table 5, it can be observed that the type of heat source distribution has low effect in tensile and compressive, axial or hoop residual stresses. According to Table 3, it can be observed that there is no change in material properties for SUS304 at temperaturesmore than 1500°C, thereforeat the temperatures greater than 1500°C, for all types of heat source distribution the stress distribution at heat affected zone is almost similar and the residual stresses are the same.

4.3. Effect of Latent Heat on Temperature Field and Residual Stresses of SUS304 Pipe

In this section, the effect of latent heat on temperature field and residual stresses was investigated.

4.4. Effect of Latent Heat on Temperature Field

The temperature-time history of Goldak heat flux distribution model on weld line with and without latent heat consideration, during the second welding pass isshown in Fig. 10, and compared with experimental results [1]. Also in Table 6, the magnitude of maximum temperature of pipe for this two conditions iscompared with experimental results [1]. From Table 6, it is clear that the value of maximum temperature when the latent heat is considered has more consistency with experimental results. In addition, it can be observed that in Goldak heat source distribution without consideration of latent heat, magnitude of maximum temperature is increased by 52°C. Therefore without considering effect of latent heat, difference between numerical results and experimental results increases.

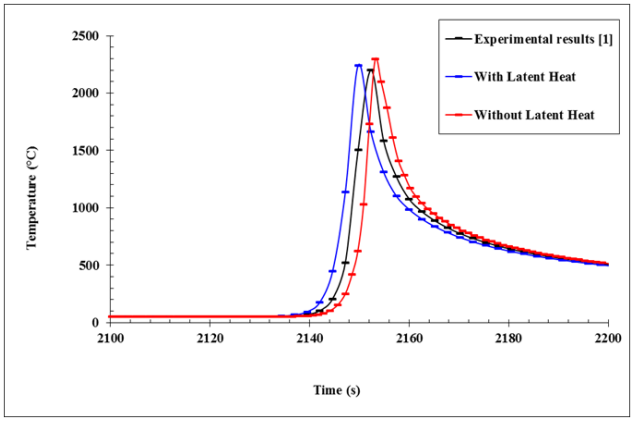

Fig. 10. Temperature history of Goldak model with body distribution with considering effect of latent heat and without it, during second welding pass on weld line.

Table 6
Effect of latent heat on maximum temperature of weld line during second welding pass in Goldak heat flux distribution.

	Maximum temperature (°C)
Goldak distribution with consideration the effect of latent heat	2242
Goldak distribution without consideration effect of latent heat	2294
Experimental result [1]	2200

4.5. Effect of Latent Heat on Residual Stresses of SUS304 Pipe

In Table 7, the values of tensile and compressive, axial and hoop residual stresses on the outside (OD) and inside (ID) surfaces of pipe for Goldak heat flux distribution with and without latent heat consideration are shown.

From the results of residual stresses presented in Table 7, it can be observed that the effect of latent heat on the maximum axial and hoop residual stresses on weld lineis negligible.

Table 7
Effect of latent heat on residual stresses.

	TAS-ID (MPa)	CAS-ID (MPa)	THS-ID (MPa)	CHS-ID (MPa)	TAS-OD (MPa)	CAS-OD (MPa)	THS-OD (MPa)	CHS-OD (MPa)
Goldak with latent heat	361	-124	422	-172	137	-379	30.2	-179
Goldak without latent heat	3607	-126	423	-171	138	-378	30.8	-179

5. Effects of Heat Flux Type on Temperature Field and Residual Stress

The heat input to the work piece during arc welding can be divided into two portions, including the heat of the welding arc, and the other is that of the melt droplets. The heat of the welding arc was modeled by a surface heat source with a Gaussian distribution that was presented by Pavelic et al. [10], and the heat of melt droplets was modeled by a volumetric heat source with uniform density presented by Goldak [9].

In this section, four types of heat flux source distribution were investigated. In the first state heat flux is assumed fully-volumetric then other three states were assumed 20% surface-80% body, 40% surface-60% body and 90% surface-10% body.

5.1. Effect of Heat Flux Type on Temperature Field

In Fig. 11, temperature history for above four types of heat flux source distribution is compared with experimental results [1] during first welding pass on inside surface of pipe at distance 3mm from weld bead at angle of 180°.

From Fig. 11, it can be observed that with decreasing percentage of body heat flux and increasing surface heat flux, maximum temperature has been reduced. More over it can be concluded that by using fully-volumetric heat source flux, the temperature history has more consistency with experimental results than the other heat source distribution. The maximum temperature of 90% surface-10% body heat flux distribution decreased 36% comparing with experimental results.

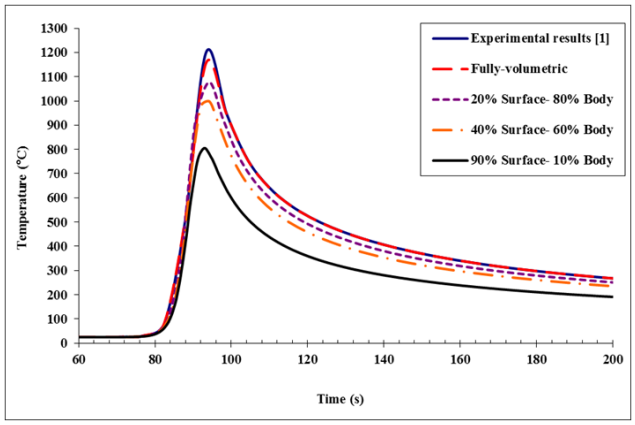

Fig. 11. Temperature history for four types of heat flux source distribution in comparison with experimental results during first welding pass on inside surface of pipe at distance 3mm from weld bead at angle 180°.

5.2. Effect of Heat Flux Type on Residual Stresses

In Figs. 12-15, the axial and the hoop residual stresses distribution on the inside and outside surfaces of pipe along the axial direction for four types of heat flux distribution are compared with experimental results.

From these figures it can be observed that with decreasing percentage of body heat flux and increasing surface heat flux the difference between numerical simulation and experimental results for predicting of hoop and axial residual stresses has been increased. Also, from Figs. 12 and 14 it is clear that specially on the weld zone, there are no important differences of axial residual stresses with decreasing percentage of body heat flux and increasing surface heat flux.

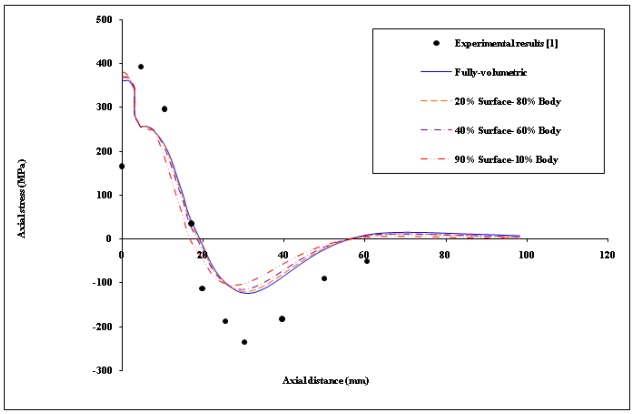

Fig. 12. Axial residual stress distribution for four types of heat flux distribution along axial distance at angle 180° on the inside surface of pipe.

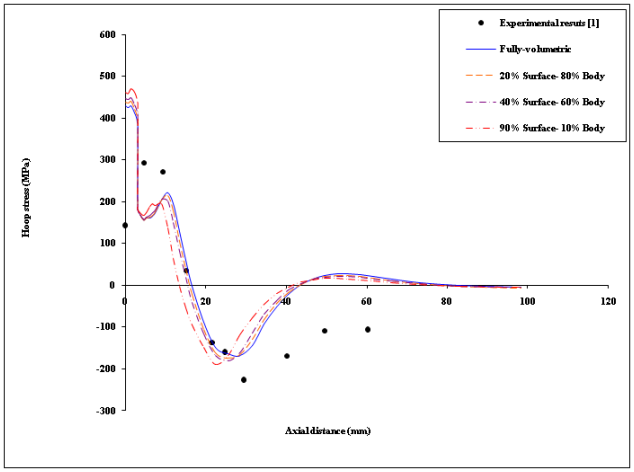

Fig. 13. Hoop residual stress distribution for four types of heat flux distribution along axial distance at angle 180 on the inside surface of pipe.

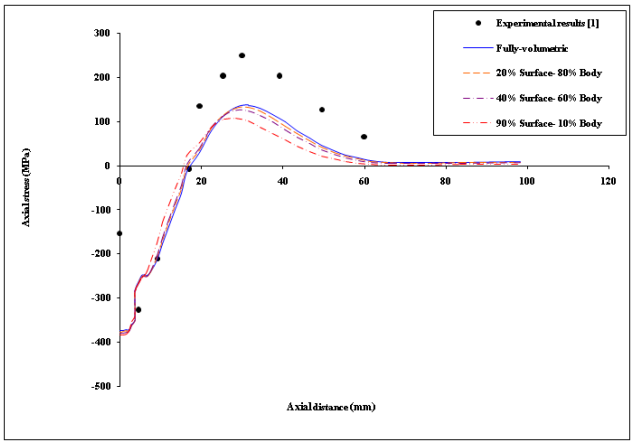

Fig. 14. Axial residual stress distribution for four types of heat flux distribution along axial distance at angle 180° on the outside surface of pipe.

From Fig. 15, it can be seen that in the welded zone compressive hoop residual stresses on the outside surface changes to tensile hoop residual stresses with increasing percentage of surface heat flux.

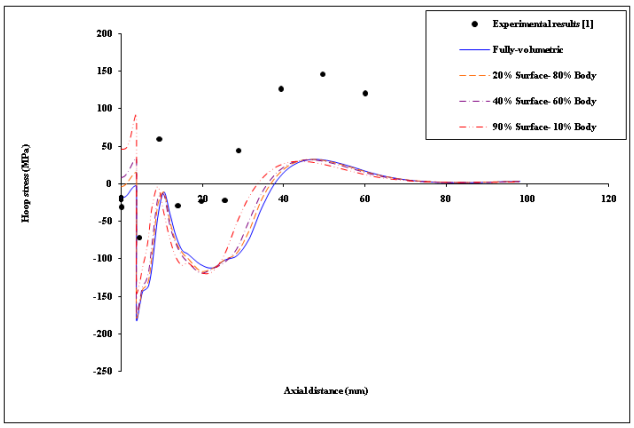

Fig. 15. Hoop residual stress distribution for four types of heat flux distribution along axial distance at angle 180° on the outside surface of pipe.

6. Conclusions

In this paper, a sequentially coupled 3D thermal-mechanical FE method was developed to predict welding residual stress distribution and temperature field during two-pass tungsten inert gas arc welding in a butt-welded stainless steel pipe. Also the effects of heat flux distribution, latent heat, and heat flux type on temperature field and residual stresses were investigated. According to the simulated results, the following conclusions can be drawn:

1. The thermal history, axial and hoop residual stresses from FE simulations had good agreement with available experimental results.

2. Three distributions of heat source including, Goldak, elliptical, and spherical heat source flux were investigated in this paper, the maximum temperature on weld line predicted by Goldak heat source flux distribution had good consistency with experimental results. Also, the type of heat source distribution had low effect in tensile and compressive axial and hoop residual stresses.

3. In simulation presented in this paper, without considering effect of latent heat the maximum temperature on weld line would increase by 5% approximately and the difference between numerical results and experimental results would-increase. Also the effect of latent heat parameter on residual stress distribution was negligible.

4. The temperature history predicted by fully-volumetric heat source flux had good agreement with experimental results. Also, with decreasing percentage of body heat flux and increasing surface heat flux, the maximum temperature on

weld line was decreased and the difference between numerical simulation and experimental results for predicting of hoop and axial residual stresses increased.

5. The change of axial residual stresses along axial direction with decreasing percentage of body heat flux and increasing surface heat flux were negligible.

6. In the weld zone, compressive hoop residual stresses on the outside surface changed to tensile hoop residual stresses with increase in percentage of surface heat flux.

References

[1] D. Deng, H. Murakawa, Numerical simulation of temperature field and residual stress in multi-pass welds in stainless steel pipe and comparison with experimental measurements, Comp. Mater. Sci., 37(3) (2006) 269-277.

[2] B. Brickstad, B.L. Josefson, A parametric study of residual stresses in multi-pass butt-welded stainless steel pipes, Int. J. Pres. Ves. Pip., 75(1) (1998) 11-25.

[3] T. Tso-Liang, C. Peng-Hsiang, T. Wen-Cheng, Effect of welding sequences on residual stresses, Comput. Struct., 81 (2003) 273-286.

[4] C.H. Lee, K.H. Chang, Three-dimensional finite element simulation of residual stresses in circumferential welds of steel pipe including pipe diameter effects, Mat. Sci. Eng., A 487 (2008) 210-218.

[5] I. Sattari-Far, M.R. Farahani, Effect of the weld groove shape and pass number on residual stresses in butt-welded pipes, Int. J. Pres. Ves. Pip., 86 (2009) 723-731.

[6] Feli S., M. E. Aalami Aleagha, M. Foroutan, E. Borzabadi Farahani, Finite element simulation of welding sequences effect on residual stresses in multipass butt-welded stainless steel pipes, J. Press. Vessel. Technol., 134(1) (2012) **9** 011209.

[7] M. Foroutan, M. E. Aalami-Aleagha, S. Feli, S. Nikabadi, Investigation of hydrostatic pressure effect on the residual stresses of circumferentially butt-welded steel pipes, J. Press. Vessel. Technol., 134(3) (2012) **4** 034503.

[8] Dean Deng, FEM prediction of welding residual stress and distortion in carbon steel considering phase transformation effects, Mater. Des., 30 (2009) 359-366.

[9] A. Goldak John, M. Akhlaghi, Computational Welding Mechanics, Springer Science, 2005.

[10] V. Pavelic, R. Tanbakuchi, O.A. Uyehara, P. S. Myers, Experimental and computed temperature histories in Gas Tungsten Arc Welding of thin plates, Weld. J., 48(7) (1969) 295-305.